Submitted, accepted and published in
Biosensors & Bioelectronics 54, 553-557 (2014); DOI: 10.1016/j.bios.2013.11.053

Graphene-based potentiometric biosensor for the immediate detection of living bacteria

Rafael Hernández[a], Cristina Vallés[b], Ana M. Benito[b],

Wolfgang K. Maser[b], F.Xavier Rius[a], Jordi Riu[a]*

[a]Department of Analytical and Organic Chemistry. Universitat Rovira i Virgili

Campus Sescelades, c/ Marcel·lí Domingo s/n, 43007 - Tarragona, Spain.

e-mail: jordi.riu@urv.cat

[b]Department of Chemical Processes and Nanotechnology

Instituto de Carboquímica ICB-CSIC, Zaragoza, Spain

Abstract. In this communication we present a potentiometric aptasensor based on chemically modified graphene (transducer layer of the aptasensor) and aptamers (sensing layer). Graphene oxide (GO) and reduced graphene oxide (RGO) are the basis for the construction of two versions of the aptasensor for the detection of a challenging living organism such as *Staphylococcus aureus*. In these two versions, DNA aptamers are either covalently (in the GO case) or non-covalently (in the RGO case) attached to the transducer layer. In both cases we are able to selectively detect a single CFU/mL of *Staphylococcus aureus* in an assay close to real time, although the noise level associated to the aptasensors made with RGO is lower than the ones made with GO. These new aptasensors, that show a high selectivity, are characterized by the simplicity of the technique and the materials used for their construction while offering ultra-low detection limits in very short time responses in the detection of microorganisms.

Keywords: aptamer, bacteria, graphene, biosensor

1. INTRODUCTION

In this communication we report for the first time a potentiometric biosensor based on chemically modified graphene and aptamers for the rapid, selective and ultrasensitive detection of *Staphylococcus aureus* (*S. aureus*). Without need for tedious pretreatment procedures, such as DNA extraction, and with a detection limit of only one colony-forming unit (CFU)/mL on a timescale of a few seconds this biosensor largely outperforms existing detection methods in simplicity and performance parameters thus demonstrating a high potential for the detection of challenging microorganisms.

Effective prevention of infectious diseases caused by bacteria is one of the major public concerns. Standard methods used to assess the presence of microbiological threats consist of specific enrichment media to separate, identify, and count bacterial cells. Depending on the specific microorganism to detect, one day to several weeks might be necessary to determine its presence. Current research efforts led to rapid detection of ultra-low amounts of microorganisms. For instance methods based on ultrafast polymerase chain reaction (PCR) (Banada et al., 2012) can detect bacteria in a few minutes with limits of detection of a few CFU. However, the techniques based on nucleic acid sequences detection usually require preprocessing steps for DNA extraction, amplification and detection, what makes the overall procedure expensive and complicated. Other recent strategies are based on the use of functionalized gold nanoparticles that bind to the bacterial surface for colorimetric detection (Wang et al., 2012), positron emission tomography (PET) imaging (Panizzi et al., 2011) or bacteriophage amplification coupled with mass spectrometry (Pierce et al., 2011). Again, in all cases this is achieved by employing tedious pretreatment steps or requires expensive equipments.

Electrochemical techniques are usually much simpler and non-expensive, and a few amperometric techniques for *S. aureus* detection have been reported so far but with

detection limits ranging between 10^6 CFU/mL in 3 hours (Morales et al., 2007) or 10^3 CFU/mL in 50 minutes (Escamilla-Gómez et al., 2008). We recently presented carbon nanotube and aptamer-based potentiometric biosensors in which we took benefit of the excellent recognition ability of aptamers towards a specific target and of the outstanding transducer abilities of carbon nanotubes. Taking benefit of the simplicity and low-cost instrumentation of potentiometric techniques, these biosensors based on aptamers (also known as aptasensors) and carbon nanotubes are able to detect, with inter and intra-strain selectivity 1 CFU of *Salmonella* Typhi in 5 mL of buffered sample in less than 1 minute (Zelada-Guillén et al., 2009), or 12 CFU of *Escherichia coli* in 2 mL of milk in a couple of minutes (Zelada-Guillén et al., 2010). Using these carbon nanotube-based aptasensors in case of challenging microorganisms such as *S. aureus* we were able to detect $8x10^2$ CFU/mL of living *S. aureus* in a couple of minutes (Zelada-Guillén et al., 2012). This value is very high compared to the cases of *Salmonella* Typhi or *Escherichia coli*. However, taking into account the inherent difficulty for the detection of *S. aureus* due to the presence of a thick polysaccharide layer of poly-N-acetylglucosamine on its surface and the low abundance of antigens externally exposed, the value of $8x10^2$ CFU/mL represents a benchmark for the direct detection of *S. aureus* employing electrochemical biosensing systems.

Herein we report the construction of a new generation of potentiometric aptasensors with significantly enhanced performance exploiting for the first time the excellent electrochemical (Ambrosi et al., 2011) and transduction (Hernández et al., 2012) properties of chemically modified graphene. Using both, graphene oxide (GO) and reduced graphene oxide (RGO) as transduction layer subsequently functionalized with a DNA aptamer able to recognize epitopes on the surface of *S. aureus* (Cao et al., 2009) we demonstrate that the resulting aptasensors are able to selectively detect just one single CFU/mL of the challenging *S. aureus* in 1-2 minutes. The ultrasensitive performance of this

potentiometric aptasensor not only outperforms results obtained with carbon nanotubes as transduction layer but represents an important breakthrough towards rapid zero-tolerance microbiological detection systems.

2. EXPERIMENTAL PART

2.1 Construction of the biosensor

The biosensor was built on top of a glassy carbon (GC) rod (length 50 mm and diameter 3 mm) jacketed with a teflon layer. The surface of the GC rod was polished first with a sheet of abrasive paper (Buehler Carbimet 600/P1200) and then with different grain-sized alumina (30, 5, 1 and 0.5 μm). Graphite oxide was prepared using a modified Hummer´s method from graphite powder (Sigma-Aldrich) by oxidation with $NaNO_3$, H_2SO_4 and $KMnO_4$ in an ice bath as reported in detail elsewhere (Hummers and Offeman, 1958). A suspension of graphene oxide (GO) sheets was obtained by sonication of the prepared graphite oxide powder in distilled water (1 mg/mL) for 2 hours, followed by mild centrifugation of the suspension at 4500 rpm for 60 min (Vallés et al., 2011). The resulting brown-coloured water dispersion with a concentration of 0.3 mg/mL contained single to few-layered GO sheets of 2 to 10 individual layers. GO films on glassy carbon (GC) electrodes were prepared as follows. Homogeneous aqueous GO dispersions of a controlled volume of 15 μL were drop-casted onto clean and polished surfaces of the GC electrodes and allowed to dry at room temperature. The deposition process was repeated other 9 times until the final thickness obtained for 10 depositions was 1460 nm (thicknesses measured by confocal microscopy). A set of GO electrodes was kept for later covalent functionalization and in another set GO was reduced to RGO for further non-covalent functionalization. Reduction of deposited GO films was performed by a 24h exposure of electrodes to hydrazine monohydrate vapours (Robinson et al., 2008). This reduction method efficiently removes various oxygen functional groups of the graphene oxide sheets and restores the aromaticity of the carbon network, even for films as thick as

1500 nm (Vallés et al., 2011). This procedure thus transforms the GO films into reduced graphene oxide (RGO) films with remaining oxygen and nitrogen moieties of about 10 % and 1.5 %, respectively. Finally, both sets of electrodes (GO and RGO electrodes) were properly functionalized with the corresponding aptamers. GO electrodes were introduced in a solution of 100 nmol of N-(3-dimethylaminopropyl)-N'-ethylcarbodiimide hydrochloride (EDC) and 25 nmol of N-hydroxysuccinimide (NHS) in a 50 mM 2-(N-morpholino) ethanesulfonic acid (MES) buffer at pH 5 for 30 min to activate the carboxylic groups present at the edge planes and defects of the deposited graphene oxide. After this step, electrodes were immersed overnight into 0.5 ml of a 1 μM *Staphylococcus aureus* SA20 binding aptamer solution dispersed in PBS pH 7.4 (1mM). In the case of the RGO electrodes, non-covalent functionalization of the *Staphylococcus aureus* SA31 binding aptamer was done depositing a drop of the 1 μM aptamer dispersed in PBS pH7.4 (1 mM) and leaving overnight in a wet atmosphere. Both 88-mer aptamers (SA20 and SA31) have similar affinities for *S. aureus* (Cao et al., 2009).

2.2 Potentiometric measurements

Potentiometric analysis was performed by real-time measurements of the electromotive force (EMF) between the terminals of a two-electrode system consisting of the GO/RGO aptasensor as the working electrode, and a double junction reference electrode (Ag/AgCl/KCl 3 M containing a 1 M LiAcO electrolyte bridge, type 6.0729.100, Metrohm AG, Herisau, Switzerland) as the reference electrode at isothermal conditions (22 ± 0.5 °C) in a water-jacketed glass cell under constant stirring conditions (300 rpm). A high-input impedance voltmeter (1015 Ω, model EMF-16, Lawson Laboratories Inc, Malvern, PA, USA) was used in all the cases to measure the difference in electromotive force. The changes on EMF were automatically measured at periods of 10 seconds. The electrolyte used in the cell was 5 mL of PBS 1.7 mM pH 7.4. The EMF value was recorded automatically with the software provided by the company. In all cases, the amount of

bacteria detected by the potentiometric measurements was simultaneously standardized in quintuplicate using the agar plate count technique.

Details about materials, aptamers, culture conditions and characterization of GO and RGO films can be found in the Supporting Information.

3. RESULTS AND DISCUSSION

The basis of the aptasensor is the transduction layer formed by GO that is deposited onto the polished surface of a GC rod. For comparison purposes, and in order to look for the best strategy of detection, two different methods of functionalization were used to attach the aptamers to this transduction layer: a covalent approach and a non-covalent one (Figures 1a-b). The covalent approach consisted of chemically linking the aptamers to GO by amide bonds formed between the carboxylic groups present on the deposited GO flakes and an amine moiety introduced at the 3' end of the aptamer by well-known carbodiimide mediated chemistry (Jung et al., 2004). The flexibility of the aptamer chains then facilitates their flat arrangement on the GO surface (comparable to DNA wrapping on carbon nanotubes (Liu et al., 2010)). In the non-covalent approach we first reduced GO to RGO to remove the unnecessary presence of the various functional oxygen moieties located on the basal and edge plane of GO. Subsequently, pyrenil moieties previously introduced at the 3' end of the aptamer were non-covalently physisorbed onto the RGO surface. Effective π-π interactions between pyrene and graphene also facilitate a flat organization of the aptamer to the RGO surface (Liang et al., 2009). In presence of the target bacteria, for both the covalent and the non-covalent functionalization, the aptamer prefers to bind to the bacteria rather than remaining attached onto the GO/RGO surface. It thus overcomes the strong π-π interactions and tends to separate its negatively ionized phosphodiester groups at a pH value of 7.4 from the underlying GO/RGO surface. Since the GO/RGO films act as asymmetric capacitors (Hernández et al., 2012) this separation of

charges provokes a subsequent change of the recorded potential.

Consecutive additions of increasing amounts of living *S. aureus* in phosphate buffer solutions (PBS, 1.7 mM, pH=7.4) were performed to test the response of the covalent and the non-covalent functionalized aptasensors. Figure 1c shows a transmission electron microscopy (TEM) image of a single *S. aureus* cell captured on the graphene-aptamer layer. The amount of bacteria in each addition was simultaneously checked by five independent measurements using the agar plate count technique. Figure 2a reveals that the non-covalent functionalized aptasensors are able to detect 1 CFU/mL in a few minutes and that an immediate change was observed after the addition of *S. aureus* for the whole working range.

For the covalent functionalized aptasensors the potentiometric response exhibits a (somewhat) higher noise level although the aptasensor is also able to respond to low additions of *S. aureus*. The difference in noise can be observed in the instrumental limit of detection (defined as three times the standard deviation of the noise), which corresponds to 29 μV for the non-covalent functionalization and 76 μV for the covalent functionalization. Both values are significantly better than the instrumental limit of detection of 240 μV obtained for carbon nanotube-based aptasensors (Zelada-Guillén et al., 2009). The lower noise and therefore the lower instrumental limit of detection for the non-covalent functionalization may be attributed to the lower number of defects in the RGO layers after hydrazine reduction (compared to the defects in the GO layers used in the covalent functionalization). This positively affects the charge-separation mechanism and favours the asymmetric capacitor-like behaviour of the transducer layer (Hernández et al., 2012) thus resulting in an overall enhanced transducer efficiency. Surprisingly, and despite a higher noise level, the precision associated with the determination of *S. aureus* using different aptasensors is better in case of the covalent functionalization approach. Figures 2b-c clearly show that the construction of a set of covalently functionalized

aptasensors offers a higher reproducibility compared to the non-covalently functionalized ones. The fact that in the case of the non-covalent functionalization an additional reduction step is required (to convert GO into RGO) may negatively impact on the reproducibility because of the inherent experimental variability due to this extra step. In any case, thick layers of transducer films (i.e. 1460 nm) help to overcome this problem (Hernández et al., 2012). At higher amounts of bacteria, each EMF increase was less prominent, demonstrating progressive saturation of the available binding sites. Although the noise level may hinder in some cases (especially in the non-covalent functionalization) a precise quantification of *S. aureus* until a better reproducibility in the home-made construction of the biosensor is attained, the biosensor can also be used for semiquantitative purposes or to decide the presence/absence of *S. aureus* below or above a threshold value (even if this threshold is as low as a few CFU/mL). It is important to remark that the apparent low values of the sensitivities (Figure 2) are due to the particular sensing mechanism, different from the classical Nernstian model, in which the change in the electromotive force results from a rearrangement of the electrical charges at the surface of GO/RGO during the recognition event. Therefore, no Nernstian responses are expected in these aptasensors.

Interestingly, when using carbon nanotubes as the transducer material (Zelada-Guillén et al., 2009) for the detection of the same microorganism the differences between the covalent and the non-covalent functionalization are tremendous: the best results (a high detection value of $8x10^2$ CFU/mL of *S. aureus*) are obtained with the covalent functionalization, obtaining a very poor detection ability with the non-covalent strategy (concentrations above 10^7 CFU/mL). This effect most likely is related to the surface properties of the aptasensor. While the entangled network of carbon nanotubes forming the transducer layer sterically reduces the interaction possibilities with the pyrene molecules, the bi-dimensional graphene sheets provides a large surface area to favour π-π stacking between RGO and pyrene moieties. This also directly influences the transducing

properties and leads to significantly improved responses for graphene-based aptasensors, independently if covalently or non-covalently functionalized.

The new aptasensors show a high degree of selectivity since no response was obtained for experiments using either *Escherichia coli* as a Gram-negative bacteria or *Lactobacillus casei* as a Gram-positive microorganism (Figures 3a-d). Control experiments (Figures 3e-i) confirmed that the responses are solely caused by the binding event between *S. aureus* and the aptamer and the subsequent transduction of the GO or RGO layer. We tested glassy carbon electrodes without transduction and recognition layer (Figures 3e) and glassy carbon (without transduction layer) both covalently and non-covalently functionalized (Figures 3f-g). We also examined the potentiometric response without recognition layer (Figures 3h) and using a non-covalently functionalized aptasensor but without pyrenil moieties (Figure 3i). There was no potentiometric response under any of these conditions, showing that the EMF change is only generated when aptamers attached to GO/RGO interact with *S. aureus*. Therefore, the two elements, aptamer (as recognition layer) and GO or RGO (as transduction layer), are essential to successfully detect *S. aureus*.

The aptasensors can be easily regenerated after each set of measurements by dissociating the aptamers from the bacteria in 2M NaCl solution for 1 hour. In presence of 2M NaCl, the tertiary structure of the aptamer changes so that *S. aureus* dissociate from aptamers. After regeneration, all the electrodes were washed gently with MilliQ water and stored in sterile PBS solution (1.7 mM, pH 7.4) for new measurements. All the electrodes were reused at least three times during around one month without any change in sensitivity or instrumental noise.

4. CONCLUSIONS

In this communication we present a graphene-based aptasensor that is able to

selectively detect a single CFU/mL in an assay close to real time of a challenging living organism such as *S. aureus*. Two different strategies were followed to attach the aptamer to the GO or RGO layer. Both, the outperforming results obtained, as well as the simplicity of the technique and the materials used for the construction of the aptasensors may pave the way towards a new generation of microbiological analysis systems characterized by construction simplicity while offering ultra-low detection limits and close to real-time responses.

To use this aptasensor in real samples with complex matrices, we would probably need to use a filtration protocol (Zelada-Guillén et al., 2010) to remove the undesired electroactive species within the original matrix, which otherwise may lead to inaccurate results in biosensing experiments. These experiments with real biological samples are foreseen and they will show the final viability of our concept. In any case it is important to remark that this filtration protocol is carried out using standard commercial cellulose acetate filters and that the total time of this step is only of 1-2 minutes.

ACKNOWLEDGEMENTS

The authors acknowledge the financial support from the Spanish Ministry of Science and Innovation (MICINN) through project grants CTQ2010-18717, MAT2010-15026, CSIC under project 201080E124 and the Government of Aragon and the European Social Fund under project DGA-FSE-T66 CNN.

REFERENCES

Ambrosi, A., Bonanni, A., Sofer, Z., Cross J.S., Pumera, M., 2011. Chemistry-A European Journal 17, 10763-10770.

Banada, P.P, Chakravorty, S., Shah, D., Burday, M., Mazzella F.M, Alland, D., 2012. PLoS One 7, e31126.

Cao, X., Li, S., Chen, L., Ding, H., Xu, H., Huang, Y., Li, J., Liu, N., Cao, W., Zhu, Y., Shen B., Shao, N., 2009. Nucleic Acids Research 37, 4621-4628.

Escamilla-Gómez, V., Campuzano, S., Pedrero M., Pingarrón, J.M., 2008. Analytical and Bioanalytical Chemistry 391, 837-845.

Hernández, R., Riu, J., Bobacka, J., Vallés, C., Jiménez, P., Benito, A.M., Maser W.K., Rius, F.X., 2012. Journal of Physical Chemistry C 116, 22570-22578.

Hummers, W.S., Offeman, R.E., 1958. Journal of the American Chemical Society 80, 1339.

Jung, D.H., Kim, B.H., Ko, Y.K., Jung, M.S., Jung, S., Lee, S.Y., Jung, H.T., 2004. Langmuir 20, 8886-8891.

Liang, Y., Wu, D., Feng, X., Müllen, K., 2009. Advanced Materials 21, 1679-1683.

Liu, J., Li, Y., Li, Y., Li, J., Deng, Z., 2010. Journal of Materials Chemistry 20, 900-906.

Morales, M.D., Serra, B., Guzmán-Vázquez de Prada, A., Reviejo, A.J., Pingarron, J.M., 2007. Analyst 132, 572-578.

Panizzi, P., Nahrendorf, M., Figueiredo, J.L., Panizzi, J., Marinelli, B., Iwamoto, Y., Keliher, E., Maddur, A.A., Waterman, P., Kroh, H.K., Leuschner, F., Aikawa, E., Swirski, F.K., Pittet, M.J., Hackeng, T.M., Fuentes-Prior, P., Schneewind, O., Bock P.E., Weissleder, R., 2011. Nature Medicine 17, 1142-1146.

Pierce, C.L., Rees, J.C., Fernández, F.M., Barr, J.R., 2011. Analytical Chemistry 83, 2286-2293.

Robinson, J.T., Perkins, F.K., Snow, E.S., Wei, Z., Sheehan, P.E., 2008. Nano Letters 8, 3137-3140.

Vallés, C., Núñez, J.D., Benito, A.M., Maser, W.K., 2011. Carbon 50, 835-844.

Wang, J., Gao, J., Liu, D., Han, D., Wang, Z., 2012. Nanoscale 4, 451-454.

Zelada-Guillén, G.A., Riu, J., Düzgün, A., Rius, F.X., 2009. Angewandte Chemie International Edition 48, 7334-7337.

Zelada-Guillén, G.A., Bhosale, S.V., Riu, J., Rius, F.X., 2010. Analytical Chemistry 82, 9254-9260.

Zelada-Guillén, G.A., Sebastián-Ávila, J.L., Blondeau, P., Riu J., Rius, F.X., 2012. Biosensors and Bioelectronics 31, 226-232.

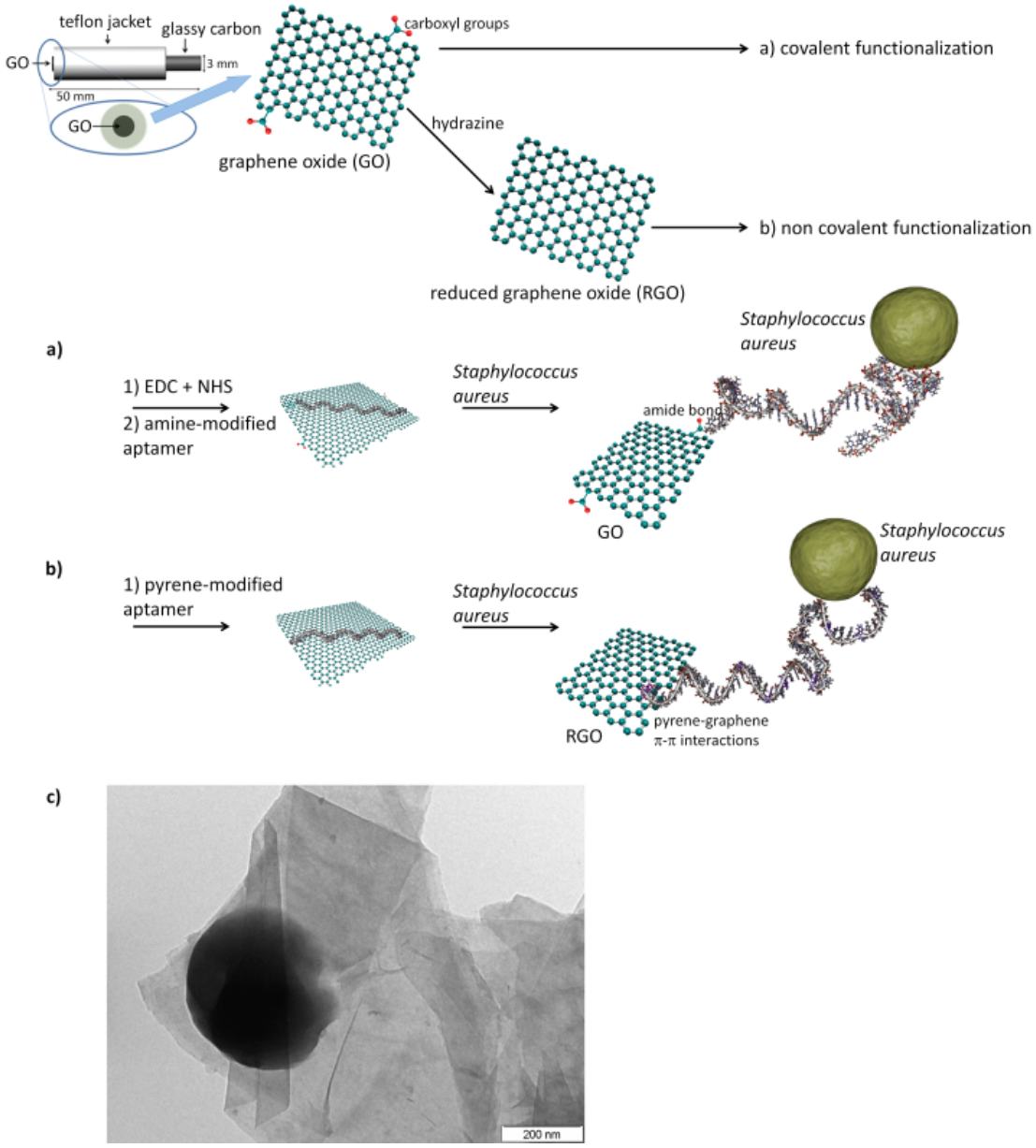

Figure 1. Scheme of the overall process of functionalization and detection of *Staphylococcus aureus* (the different parts are not to scale). Top: Schematic illustration of the potentiometric aptasensor. For sake of clarity the GO layer only presents a few carboxyl groups and other functional defects (e.g. alcohols, ethers, ketones …) are not shown. a) The covalent functionalization of GO with the *S. aureus* aptamer following carbodiimide-mediated chemistry facilitates a flat stacking of the aptamer to the GO surface. b) The non-covalent functionalization of GO with the *S. aureus* aptamer results in π-π stacking between RGO and pyrene moieties and also facilitates a flat stacking of the aptamer to the RGO surface. c) TEM image of a single *S. aureus* cell captured on a graphene-aptamer layer.

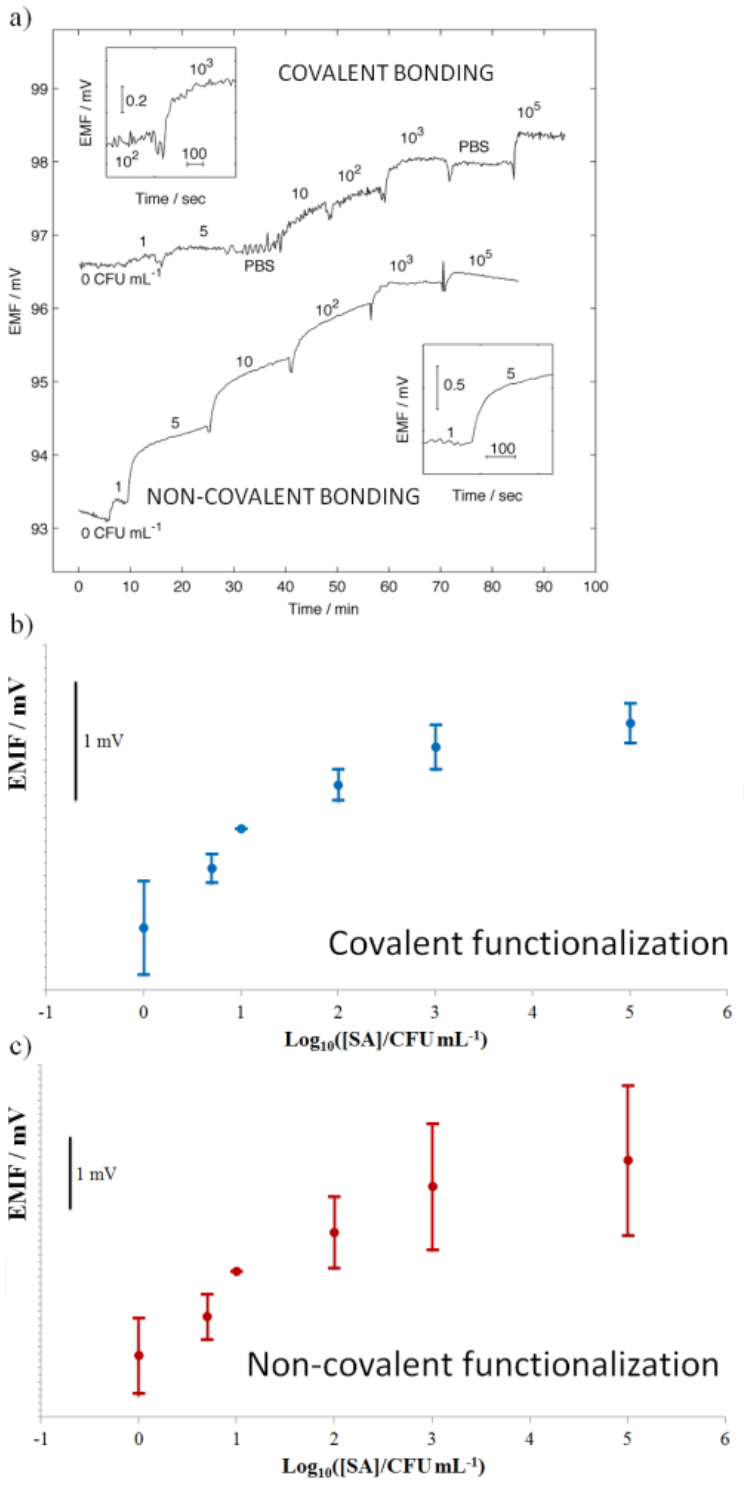

Figure 2. a) Aptamer-functionalized aptasensor exposed to stepwise increases of *S. aureus* concentration and the corresponding potentiometric response; numbers above each potentiometric jump represent the final concentration of bacteria. Insets show the detail of two inoculation steps for the covalent and non-covalent functionalization. b) EMF response versus log of concentration of *S. aureus* for the covalent functionalization. c) EMF response versus log of concentration of *S. aureus* for the non-covalent functionalization. In b) and c) error bars are standard deviation of the response obtained at a given concentration for six different sensors. The sensitivities of the aptasensors are 0.34 mV/decade (covalent functionalization) and 0.55 mV/decade (non-covalent functionalization).

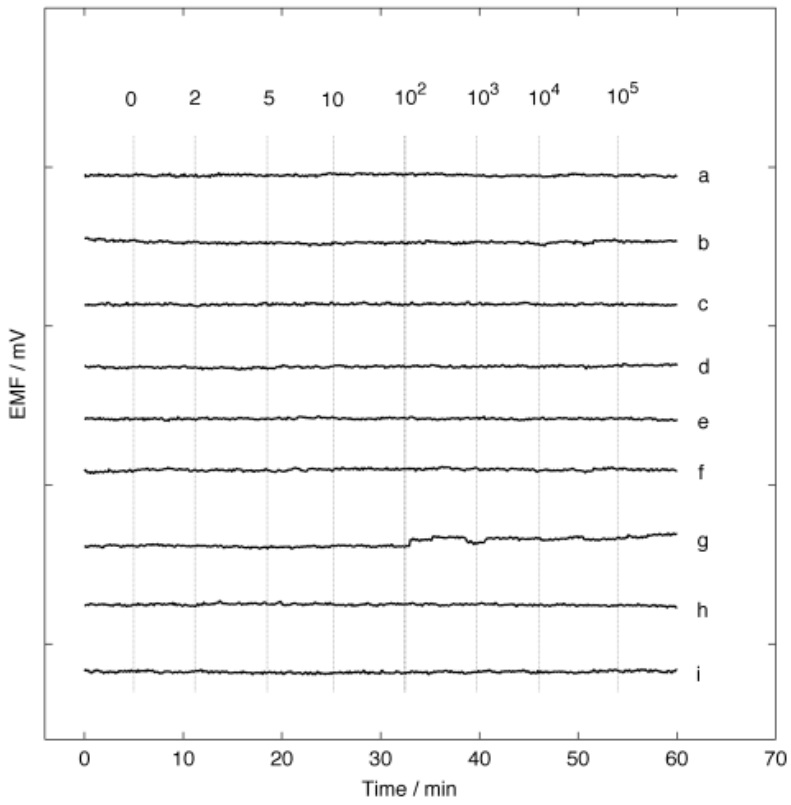

Figure 3. Selectivity (a-d) and control (e-i) assays. EMF response versus time for different concentrations of bacteria. Vertical lines represent inoculation with increasing amounts of bacteria (in CFU/mL). From top to bottom: a) and b) Covalently functionalized biosensor exposed to *Escherichia coli* and *Lactobacillus casei*, respectively; c) and d) Non-covalently functionalized biosensor exposed to *Escherichia coli* and *Lactobacillus casei*, respectively; e) Glassy carbon electrode exposed to *S. aureus*; f) and g) Glassy carbon without GO/RGO covalently and non-covalently functionalized with aptamer exposed to *S. aureus*; h) Glassy carbon with a layer of GO/RGO and without aptamer exposed to *S. aureus*; i) Non-covalently functionalized aptasensor without pyrenil moieties in the aptamer exposed to *S. aureus*.

Supporting Information

Graphene-based potentiometric biosensor for the immediate detection of living bacteria

*Rafael Hernández, Cristina Vallés, Ana M. Benito, Wolfgang K. Maser, F. Xavier Rius, and Jordi Riu**

Reagents and apparatus: Graphene powder, sodium nitrate, sulphuric acid, potassic permanganate, hydrazine hydrate, N-hydroxysuccinimide (NHS), 2-(N-morpholino) ethanesulfonic acid (MES) and N-(3-dimethylaminopropyl)-N'-ethylcarbodiimide hydrochloride (EDC) were purchased from Sigma-Aldrich. Aqueous solutions were prepared with freshly deionized water (18.2 MΩ·cm specific resistance) obtained with a Milli-Q PLUS reagent-grade water system (Millipore). Sand papers and alumina were obtained from Buehler. Glassy carbon rods 3 mm diameter was purchased from HTW GmbH. *Staphylococcus aureus* binding aptamer SA20 with the sequence 5'-GCAAT GGTAC GGTAC TTCCG CGCCC TCTCA CGTGG CACTC AGAGT GCCGG AAGTT CTGCG TTATC AAAAG TGCAC GCTAC TTTGC TAA-3' modified in the 3' end with a 3C spacer followed by a pyrene cap phosphoramidite was purchased from Eurogenetec (London, UK). The same company provide the *Staphylococcus aureus* binding aptamer SA31 with the sequence 5'-GCAAT GGTAC GGTAC TTCCT CCCAC GATCT CATTA GTCTG TGGAT AAGCG TGGGA CGTCT ATGAC AAAAG TGCAC GCTAC TTTGC TAA-3' modified in the 3' end with a 6C spacer and an amine moiety (-$(CH_2)_6$-NH_2). Aliquots of aptamers were obtained and stored in the refrigerator at -80ºC until use. Lyophilized strains of *Staphylococcus aureus* (CECT 4630), *Lactobacillus casei* subsp. *casei* (CECT 4180) and *Escherichia coli* (CECT 4558) were purchased from Colección Española de Cultivos Tipo (Valencia, Spain). All the potentiometric measurements were done using a Keithley high imput impedance voltmeter M6514 (London, UK) in a thermostatized 20 ml flask (22.0 ± 0.5ºC). High-resolution transmission electronic (HR-TEM) images were taken on a FEI

Tecnai G2 20 microscope. Confocal microscopy LEICA Dual Core 3D measuring Microscope 3D equipment was used to control the thickness of graphene depositions. Atomic force microscope (AFM) images were obtained with a Multimode8 microscope with control electronics Nanoscope V (Bruker). A high input impedance electrometer 6514 from Keithley was used for potentiometric measurements. All the experiments were done at room temperature (22.0±0.1ºC) in a bath from Polyscience (ref.9106) with the same double-junction Ag/AgCl/ 3 M KCl reference electrode (type 6.0729.100, Methrom AG) containing a 1 M LiAcO electrolyte bridge. The same cell was used for the measurements in all the experiments in order to ensure that each experiment was carried out under the same conditions. X-Ray photoelectron spectroscopy (XPS) was carried out on an ESCAPlus Omicron spectrometer using a monochromatized Mg X-ray source (1253.6 eV). XPS data were analyzed using the CasaXPS software.

Culture conditions: All bacteria strains were cultivated under the same experimental conditions, including incubation time and temperature. The bacteria lyophiles were stored at -20 °C in glycerol/TSB medium (10% v/v) and reactivated by incubating the bacteria in 10 mL of sterile TSB at 37 °C for 24 h. The bacteria samples were then centrifuged at 6000 rpm for 15 minutes and the supernatant was discarded. The precipitate was successively washed with PBS 1.7 mM pH 7.4 following the same centrifugation conditions previously mentioned. The pellet was finally resuspended in sterile PBS 1.7 mM pH 7.4. The resulting solution (namely 100 solution) was sixth-fold 1:10 diluted serially to give a series of 10^{-1} to 10^{-6} stock solutions of bacteria. The stock solutions were quantified in quintuplicate using the standard plate count method (Gerhardt et al., 1981) in TSA and the same procedure was also applied to the standardization of the variable aliquots of stock solutions that were used to inoculate the samples to be analyzed. The bacteria concentration was measured in colony-forming units (CFU)/mL.

Characterization of graphene oxide and graphene oxide films on glassy carbon electrodes: Water dispersions of graphene oxide (GO) with a concentration of 0.3 mg/mL contain GO flakes comprised of few-layered GO sheets with 2 to 10 individual graphene layers with a majority of 4. Flake sizes typically range from 200 nm to 800 nm (Figure S1).

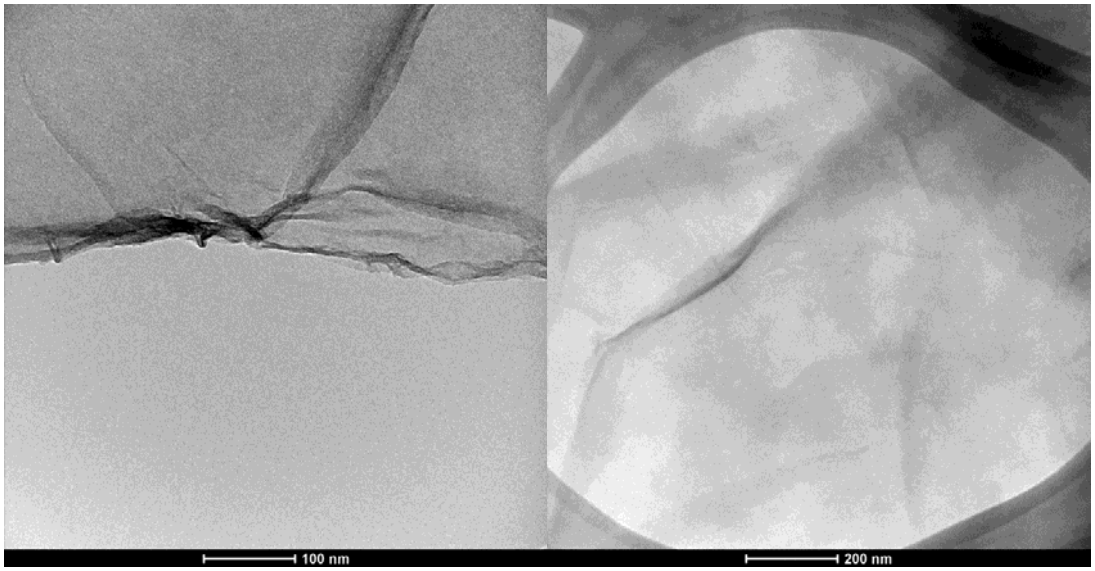

Figure S1. HRTEM images of graphene oxide

Figure S2 shows AFM images for RGO films over the GC electrode. The films present almost no agglomerates with an homogeneous and smooth coating. The surface roughness is about 30 nm.

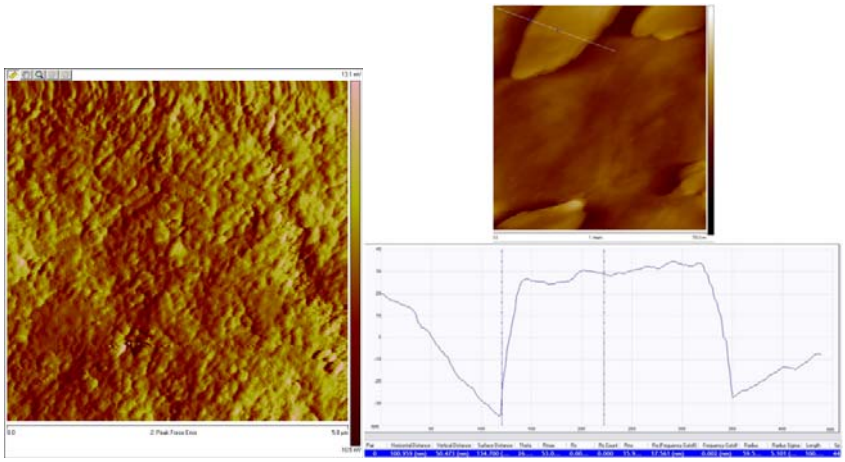

Figure S2. AFM images of RGO films on glassy carbon electrodes (left). Height profile taken exhibiting a surface roughness of about 30 nm (right).

X-ray photoelectron spectroscopy (XPS) of RGO: The chemical composition of the prepared RGO material was analyzed by XPS. The resulting C1s core electron spectrum is depicted in Figure S3. Deconvolution reveals the presence of C-C bounds at 288.2 eV, various types of oxygen functionalities C-O, C=O and O-C=O moieties at 285.8 eV, 287.5 eV and 289.5 eV, respectively. Additionally, C-N functional moieties are observed at 284.6 eV. The quantified atomic percentages for C, O and N correspond to 88.36 at. %, 10.19 at. % and 1.45 at. %. The oxygen functional groups in RGO are remaining from the starting GO material, while nitrogen groups originate from both, the use of $NaNO_3$ in the preparation of GO as well as the use of hydrazine monohydrate vapors in the reduction process Most interestingly, the appearance of the π-π contribution in the XPS spectrum at 291.6 eV, not observable in the starting GO material, indicates first hints for the restoration of carbon sp^2 character upon reducing GO to RGO.

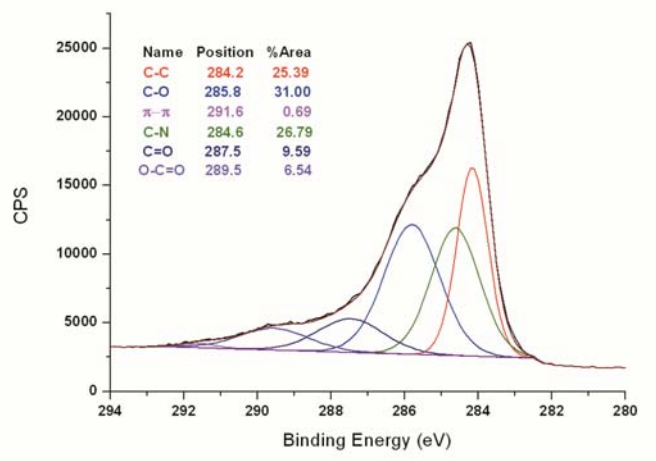

Figure S3. C1s core electron XPS of as prepared RGO

Gerhardt, P., Murray, R.G.E., Costilow, R.N., Nester, E.W., Wood, W.A., Krieg, N.R., Philips, G.B. (Eds.), 1981. Manual of methods for general bacteriology, Washington